Vulnerability of the superficial zone of immature articular cartilage to compressive injury

Bernd Rolauffs[1,2], **Carol Muehleman**[3,4,6], **Jun Li**[3], **Bodo Kurz**[5], **Klaus E. Kuettner**[3,6], **Eliot Frank**[1], and **Alan J. Grodzinsky**[1]

[1]Massachusetts Institute of Technology, Center for Biomedical Engineering, Cambridge, MA 02319, USA

[2]BG Trauma Center, Eberhard Karls University, 72076 Tuebingen, Germany

[3]Department of Biochemistry Rush University Medical Center, Chicago, IL 60612, USA

[4]Department of Anatomy and Cell Biology, Rush University Medical Center, Chicago, IL 60612, USA

[5]Department of Anatomy, Christian-Albrechts-University Kiel, Germany

[6]Department of Orthopedic Surgery, Rush University Medical Center, Chicago, IL 60612, USA

Abstract

Objective—The zonal composition and functioning of adult articular cartilage causes depth-dependent responses to compressive injury. In immature cartilage, shear and compressive modulus, collagen and glycosaminoglycan (GAG) content also vary with depth. However, there is little understanding of depth-dependent damage caused by injury. Since injury to immature knee joints most often causes articular cartilage lesions, our objectives were to characterize the zonal dependence of biomechanical, biochemical and matrix-associated changes cause by injury.

Methods—Superficial and deeper zones disks from bovine calves were biomechanically characterized, injured (50% compression, 100%/sec) and re-characterized. Tissue compaction upon injury, GAG-density, GAG loss and biosynthesis were measured. Collagen-fiber-orientation and matrix damage was assessed using histology, Diffraction-Enhanced-X-Ray-Imaging, and texture analysis.

Results—Injured superficial disks showed surface disruption, compaction by 20.3±4.3%, and immediate biomechanical impairment: dynamic stiffness decreased to 7.1±3.3% of its initial value and equilibrium modulus was below detection. Tissue areas apparently intact by histology showed clear textural alterations. Injured deeper zones disks showed collagen crimping but remained undamaged and biomechanically intact. Superficial zone disks did not lose GAG immediately after injury but lost 17.8±1.4% by 48h; deeper zones disks lost only 2.8±0.3% GAG. Biomechanical impairment was primarily associated with structural damage.

Conclusion—The soft superficial zone of immature cartilage is vulnerable to compressive injury causing superficial matrix disruption, extensive compaction, and textural alteration, and resulting in immediate loss of biomechanical function. In conjunction with delayed superficial GAG loss, these changes may predispose the articular surface to further softening, damage, and increased risk of developing secondary OA.

*To whom correspondence should be addressed: Bernd Rolauffs, M.D.; BG Trauma Center Tuebingen, Schnarrenbergstr 95, 72076 Tuebingen, Germany; Phone: +49-7071-6060; Fax: +49-7071-606-1002; berndrolauffs@googlemail.com.

Articular cartilage lesions repair insufficiently and, with damage to the subchondral bone, lead to the formation of fibrocartilage(1). The resulting repair tissue has inferior biomechanical and biochemical properties(1,2) and poorer wear characteristics(3) which frequently lead to the development of secondary osteoarthritis (OA)(4). Articular cartilage injury models have attempted to unravel relationships between mechanically induced extracellular matrix (ECM) damage and degradation, apoptosis, and proteoglycan loss after injury(5-8).

In adult articular cartilage, injury-induced damage varies with depth due to the depth-dependent nature of ECM composition(9), structure(10), and biomechanical properties(11). Fissuring of the articular surface(12), cell death(12) and impaired collagen integrity(13) occur only near the articular surface. For fetal and newborn bovine cartilage, depth-dependent ECM variations of compressive and shear moduli, collagen and glycosaminoglycan (GAG) content have also been reported(14,15). However, after compressive injury, damage-associated changes in depth-dependent characteristics of ECM are not known. It is not clear if variations in ECM composition, structure and biomechanical properties are sufficient to cause depth-dependent injurious effects in immature cartilage.

We hypothesized that since the immature articular surface is softer than the middle and deeper zones, mechanical compression injury may give rise to largely surface-confined structural damage. Such surface-confined damage could lead to an *immediate* biomechanical but *delayed* biochemical impairment of the superficial zone. Because injury to the immature knee joint causes articular cartilage lesions(16) in the majority of patients, it is critical to analyze initial depth-dependent traumatic events to better understand the progression of superficial damage of immature cartilage towards degradation, which could ultimately lead to the development of early secondary OA.

Methods

Articular Cartilage Explants and Culture

Full-thickness bovine articular cartilage explants ($\sim$2 cm^2 surface area) including the intact superficial zone, were harvested from the weight-bearing areas of medial (MC) and lateral (LC) condyles and patellofemoral grooves (G) of 1-2 week old calves within 24h of death. Explants were equilibrated in 5%CO_2 in DMEM with 10% FBS, 10nM HEPES, 1nM sodium-pyruvate, 0.1mM non-essential amino acids, 0.4mM proline, 20μg/ml ascorbic acid plus antibiotics(17).

Preparation of Superficial and Deeper Zones Cartilage Disks

To prepare disks representing the superficial and successive deeper zone, cartilage cylinders (3mm diameter) were punched prior to mechanical testing. The cylinders were sliced perpendicular to the longitudinal axis into 200–400μm-thick superficial zone disks (including the articular surface) and deeper zones disks ($\sim$1300μm). Full-thickness cartilage cylinders were punched for additional analyses but not sliced into disks.

Disk Thickness and Testing of Mechanical Properties

Disks were placed onto the bottom of a single well of a polysulfone loading chamber with an upper platen attached to an incubator-housed loading instrument(18). Thickness was measured individually in uniaxial unconfined compression by applying a slow compression ramp (20μm/sec ramp speed) with automated interrupt caused by an increase in offset load indicating contact between platen and disk.

To determine the mechanical properties, three successive displacement-controlled compression ramps to final strains of 10% (200-sec compression followed by 600-sec hold), 12.5% and 15% (30-sec compression, 300-sec hold) were applied[17] to each superficial zone disk and separately to its corresponding deeper zones disk[18] in uniaxial unconfined compression. The resulting equilibrium loads at these strains were used to compute the unconfined equilibrium moduli. At 15% final offset strain, each disk was subjected to 3% dynamic strain amplitude at 1.0/0.1Hz to compute the dynamic stiffnesses[17].

Mechanical Injury, Peak Stress, and Re-Testing of Mechanical Properties

Disks were equilibrated for 20min. Injurious compression to a final strain of 50% at 100%/sec was applied to each individual disk in uniaxial, unconfined compression. We refer to this compressive injury protocol henceforth as "injury". These injury loading parameters were chosen based on two strain- and strain-rate dose-response studies[17,19]. During injury, the peak stress was measured by the loading instrument[18]. After 5min of unconfined re-swelling, the thickness, unconfined equilibrium modulus and dynamic stiffness were re-measured.

Biochemical and Biosynthetic Analyses

After injury, disks were incubated as described, then solubilized overnight in 500μg/ml proteinase-K. sGAG content and loss to the medium were assessed using the dimethylmethylene-blue-dye-binding-assay[20]. sGAG content was determined for both control and injured disks. sGAG loss to the medium was determined after completion of biomechanical re-testing, at 24 h, and at 48h (disks were individually incubated in fresh medium). The medium was snap-frozen, lyophilized, re-suspended and analyzed as described. Before injury and 5min after injury, the pre- and post-injury GAG densities were calculated using the re-measured disk volume.

To assess biosynthesis of sGAG and total protein after injury, radiolabel incorporation was measured by incubating the disks for 24h after injury in fresh medium containing $^{35}SO_4^{-2}$ and ^3H-proline as described[19]. Disks were digested with protease-K (100μg/ml in 50mM Tris-HCl, 1mM $CaCl_2$, pH8, 18h). Digest-aliquots were analyzed in a liquid scintillation counter. Spillover-corrected data were calculated as scintillation counts/tissue volume.

Articular Cartilage Damage Score after Injury

To quantify damage, superficial and deeper zones disks and full-thickness cylinders containing both superficial and deeper zones were injured and with controls snap-frozen in liquid nitrogen, fixed in 10% paraformaldehyde and paraffin-embedded. 6μm sections were stained with Safranin-O/fast green, photographed and graded by a blinded investigator using a 5-point-scale (Figure 5E). Because both the superficial and deeper zones disks as well as full-thickness cylinders showed similar damage patterns, further analyses of the collagen fiber orientation were performed on uncut full-thickness injured and control cylinders. In addition, full-thickness injured and control cylinders were first injured, secondly DEI-imaged (see below), and then histologically analyzed.

Collagen Fiber Bundle Orientation

To assess the collagen fiber orientation, histological slides were stained with picrosirius red. Polarized images were recorded on a Nikon-Eclipse-microscope (40×). A blinded investigator performed a Fast-Fourier-Transform-analysis at 400× (Visual C++.NET) of full-thickness cylinders. For three regions of interest in the superficial and deep zones on each photomicrograph, the directionality was determined using a power spectrum for generation of an intensity histogram to show the angle distribution[21]. The power spectrum

was generated using segments that correspond to increments of one degree of orientation. The collagen fiber bundle angle was referenced to the longitudinal axis and defined as the angle at which the distribution value function was highest(21).

Diffraction-Enhanced X-Ray Imaging (DEI)

To visualize damage, full-thickness injured and control cylinders were x-rayed with Diffraction-Enhanced X-Ray Imaging (DEI). Immediately after injury, cylinders were snap-frozen in liquid nitrogen, fixed in 10% paraformaldehyde to minimize re-swelling and morphometric changes, and stored at -80°C. Cylinders were DEI-imaged at the X-15-beamline of the National-Synchrotron-Light-Source (Brookhaven National Laboratory) as described(22). Briefly, the samples were positioned for A-P imaging with a collimated fan beam of X-rays prepared by two silicon crystals. Once this beam passes through the cartilage, a third silicon crystal diffracts the X-rays onto an image-plate detector (FuJi-BAS2500).

Texture Analysis

Images of selected sections of superficial and deeper zones disks and of full-thickness cylinders as well as selected DEI-images were grey-scale-converted. The texture analyzer ImageJ-plug-in (NIH, Maryland, USA) was used to calculate texture features for selected ROIs according to their original implementation(23) to quantify local contrast and spatial distribution. In initial analyses, we applied several features, which showed that, for the present study, 3 were most valuable: angular second moment (ASM; increases with texture regularity), inverse difference moment (IDM; increases with homogeneity), and entropy (E; increases with irregularity).

Statistical Analysis

All data are presented as mean±SEM. Data were analyzed for normality with the Kolmogorov-Smirnov-test (SigmaStat-3.1). Normally distributed data were subjected to one-way-ANOVA and Holm-Sidak post-hoc-test. Non-normally distributed data were tested with ANOVA-on-Ranks and Dunn's post-hoc-test. For comparisons of two groups, Student's t-tests (matched pairs) were performed. Differences were considered significant at $p<0.05$.

Results

Pre-Injury Disk Thickness and Biomechanical Properties

The pre-injury thickness of superficial zone disks was 307±38μm and of deeper zones disks 1352±84μm (Figure 1A). The equilibrium modulus of superficial zone disks was 0.24±0.05MPa. Deeper zones disks showed a significantly higher equilibrium modulus of 0.66±0.05MPa ($p<0.001$, Figure 1B). Superficial zone disks showed a dynamic stiffness of $1.77 ± 0.77$MPa at a frequency of f=1Hz and of $1.40 ± 0.67$MPa at f=0.1Hz, while deeper zones disks demonstrated a dynamic stiffness that was higher at each frequencies ($p<0.0001$): 12.06±1.03MPa at f=1Hz and 8.13±0.78MPa at f=0.1Hz (Figure 1C). These results show a depth-dependent variation of the biomechanical properties of newborn bovine cartilage similar to adult cartilage(11) and having equilibrium moduli on the same order as previously reported(14). To assess whether differences in the disk dimensions of the thin superficial zone disks and the thicker deeper zones disks had any effect on the biomechanical properties assessed by our methods, we compared deeper zones disks ≤1010μm thick (1002±41.3μm) with deeper zones disks ≥1600 μm (1684.8±41.2μm). The equilibrium moduli of the two groups were not significantly different.

Injury Peak Stress, Post-Injurious Changes in Disk Thickness, and Post-Injurious Impairment of Biomechanical Properties

During injury, the peak stress reached in superficial zone disks (0.88±0.21MPa) was significantly lower than that in deeper zones disks (13.5±0.69MPa, *p*<0.0001, Figure 2A). The thickness after injury was significantly decreased in both superficial and deeper zones disks (*p*<0.01, Figure 2B) but the extent of compaction varied. Superficial disks were irreversibly compressed by 20.31±4.31%, whereas deeper zones disks were compressed by 7.8±0.47% (Figure 2B). We next assessed the change in biomechanical properties caused by injury. The individually re-measured equilibrium moduli of the superficial zone disks were so low that they were not resolvable, indicating a functional destruction of the tissue (Figure 2C). In strong contrast, the equilibrium moduli of all deeper zones disks were not significantly changed by injury (Figure 2C), indicating that no functional damage had occurred. The re-measured dynamic stiffness was resolvable in all disks of both zones. In superficial zone disks, the dynamic stiffness was decreased to 7.12±3.34% of the value before injury (MC *p*<0.05; LC, G *p*<0.001, Figure 2D). In deeper zones disks, the dynamic stiffness was decreased to 72.13±2.88% (MC, G *p*<0.0001, LC *p*<0.05, Figure 2D). Our results demonstrate an extensive impairment of the dynamic properties of the superficial zone.

Pre- and Post-Injury Biochemical Analyses

Superficial zone control disks contained 135.1±11.4μg GAG, whereas control disks of the deeper zones contained 408.6±55.6μg GAG (*p*<0.001, Figure 3A). When normalized by disk volume, the GAG density of superficial zone control disks (69.25±5.27μg×10^6/μm^3) was higher than that in deeper zones disks (40.57±4.52μg×10^6/μm^3, MC *p*<0.05, LC, G *p*<0.001, Figure 3B). We then calculated the GAG loss into the medium. Immediately after biomechanical characterization, GAG loss from control disks was not detectable. After 48h, superficial zone control disks lost 10.0±0.9% of their GAG content (13.6±1.3μg GAG) while deeper zone control disks lost 6.7±0.5% (26.6±1.8μg GAG, MC, G *p*<0.0001, LC *p*<0.01, Figure 3C).

Immediately after injury and subsequent biomechanical re-characterization, GAG loss to the medium was not detectable. However, by 48h after injury, superficial zone disks lost 17.8±1.4% of their GAG content (23.78±1.93μg GAG, Figure 3C), representing 1.78-fold higher levels than control non-injured disks (MC *p*<0.0001, LC *p*<0.01, G *p*<0.05). The injured deeper zones disks lost 2.8±0.3% of their GAG content (16.44±1.25μg GAG). GAG loss from deeper zones disks of the lateral condyle or patellofemoral groove was not significantly different compared to control disks. However, injured medial condyle disks demonstrated 0.53-fold lower levels of GAG loss versus controls (*p*<0.01). Thus, injury increased GAG loss from the superficial zone while GAG loss from the deeper zones was decreased or not altered by injury, demonstrating a depth-dependent variation.

We also investigated whether superficial zone GAG loss occurred during day-1 or day-2 after injury. Control disks lost significantly more GAG during day 1 versus day 2 (*p*<0.01). Injured superficial zone disks showed significantly increased amounts of GAG loss during day-1 and day-2 (day 1: 2.03-fold increase, day 2: 2.33-fold increase, MC, LC, G *p*<0.001, amounts were comparable). Thus, injury to superficial zone disks led to increased GAG loss, and the relative amounts increased over time.

Injury-related tissue compaction caused an immediate increase in GAG density in superficial disks from 67.35±7.04 to 84.15±8.84μg×10^6/μm^3, MC, LC, G *p*<0.001) and in deeper zones disks from 38.03±6.02 to 41.24±6.54 μg×10^6/μm^3, MC *p*<0.001, LC *p*<0.01, G *p*<0.05). In superficial zone disks, the increase in GAG density was more pronounced (24.95±1.19%)

than in deeper zones disks ($8.43\pm7.69\%$, Figure 3D). Collectively, these data suggest that the GAG density was more affected by tissue compaction then by GAG loss.

Pre- and Post-Injury Biosynthesis

In control disks, incorporation of ^{35}S-sulfate and ^{3}H-proline was higher in superficial than in deeper zones disks ($p<0.001$). After injury, the incorporation into both superficial and deeper zones disks was decreased, but by an amount that did not reach significance when compared to control disks (Figure 4A,B). Thus, after injury, the increased loss of GAG (see above) was not associated with an increase in biosynthesis.

Articular Cartilage Damage Score after Injury

Control samples showed no damage (Figure 5A,B), whereas 52.9% of the injured disks showed visible surface damage ranging from disruption to compaction (Figure 5C,D). In addition, some disks were ovally deformed similar to another study(24). The injured samples were graded as 1.08 ± 0.28 (range 0-3) and control samples as 0 ($p<0.05$, Figure 5E). Importantly, not all sections of a particular disk showed similar extents of the damage; for example, a surface split was visible in some but not in all vertical sections. Thus, the largest amount of damage of each individual disk was scored.

Collagen Fiber Bundle Orientation

We assessed injury-inducted changes in collagen fiber orientation. Collagen angles of control disks of the superficial zone were $79.1\pm6.2°$ and remained unchanged by injury. Collagen angles of deeper zones control disks were lower ($50.8\pm4.3°$, $p<0.01$) and, after injury, were increased to $64.4\pm4.8°$ ($p<0.01$, Figure 5F).

Texture Analysis of Histological Sections

In histological sections of control, non-injured disks, ASM and IDM were lower ($p<0.01$) and E higher ($p<0.01$) in superficial than deeper zones (Figure 5G). Thus, images of superficial zone disks were more regular (ASM) and homogeneous (IDM) and less irregular (E). Secondly, we attempted the analysis of injured disks but ROIs containing structural damage such as surface splits lost all texture information within the split (Figure 5D). Therefore, we analyzed ROIs of injured disks that appeared histologically intact to ask whether areas without histologically visible damage may nevertheless display texture changes suggesting compressive or structural damage. We showed that ASM and IDM were significantly lower ($p<0.01$) and E higher ($p<0.01$) in the superficial but not deep zones of injured disks compared to controls (Figure 5H). Thus, injury led to a significant decrease of image regularity and homogeneity and a significant increase of irregularity in ROIs without visible histological surface damage, suggesting injury-induced structural surface damage.

Diffraction-Enhanced X-Ray Imaging and DEI Texture Analysis

Not all histological sections of individual disks showed similar extents of damage or were quantifiable by texture analysis. To visualize damage to the entire superficial zone in a way that allows further quantification, selected samples were x-rayed with DEI, which can show compressive or other morphological changes of articular cartilage (22,25-28). With DEI, we visualized surface disruptions of injured disks (Figure 6A,B). That DEI indeed showed surface disruptions was confirmed by histology on the same disks that were x-rayed. Utilizing DEI-images, we were then able to quantify texture features of ROIs of injured disks containing structural surface damage that were not quantifiable by histology. We demonstrated that these regions showed a decreased ASM ($p<0.001$) and increased E ($p<0.001$, Fig. 6D) as measurements of image regularity and irregularity. IDM as

homogeneity measurement remained unchanged. Thus, DEI-images were suitable to establish texture differences between intact and superficially damaged cartilage.

Discussion

We analyzed the biomechanical, biochemical and structural characteristics of the superficial and subsequent deeper zones of immature articular cartilage and their response to compressive injury. We showed that the zonal composition of immature ECM varied to an extent that was sufficient to cause depth-dependent injurious effects similar to that in adult cartilage. Collectively our results suggest a vulnerability of the soft superficial zone to immediate biomechanical impairment, caused by structural damage, and a predisposition of this damaged surface to further softening and degradation by delayed biochemical impairment.

Our choice of compressive injury led to a complete loss of the equilibrium stiffness and a near-loss of the dynamic stiffness of the superficial but not deeper zones of immature cartilage. These results represent a depth-dependent zonal but not regional variation of the response to injury similar to adult articular cartilage because we showed that the immature articular cartilages of both condyles and the patellofemoral groove responded similarly to injury(12). However, we also demonstrate several additional effects of injury including GAG loss, changes in GAG density, a flattened collagen fiber orientation, severe structural damage such as surface disruptions, and extensive compaction. To identify the main effects of injury that appear responsible for the immediate biomechanical failure of the superficial zone, it is necessary to briefly review the interconnections of biomechanical properties and biochemical composition upon which those biomechanical functions depend.

The biomechanical properties of cartilage have been attributed primarily to its GAG and collagen constituents(29). The compressive stiffness is positively related to the GAG concentration with its fixed charge density and negatively related to tissue hydration and cellular content(14,30). Important is the osmotic swelling pressure due to the negatively charged GAG content and the collagen network resisting these pressures(31). The dynamic stiffness is primarily based on pressurized interstitial fluid due to a high resistance to fluid flow under load(32), governed by the matrix hydraulic permeability(33), which in turn depends on GAG content and fixed charge density(34), collagen fiber orientation(35), and tissue deformation(36). Thus, both the equilibrium compressive and dynamic properties depend primarily on these components.

We first analyzed GAG loss, content, and density and showed that immediately after injury, at a time when the biomechanical impairment of the superficial zone had already occurred; there was no detectable GAG loss into the media. Thus, the biomechanical impairment was recorded *before* GAG loss had occurred, and factors other than GAG loss must have caused this impairment. One could speculate that changes in the GAG density, and therefore in the fixed charge density, may lead to changes in the biomechanical properties because the fixed charge density is strongly associated with the compressive stiffness(37). During non-injurious, physiological compressions such as gait, GAG compaction leads to increased stiffness via an increased fixed charge density(38). However, immediately after compression injury, the superficial zone GAG density increased by 25% due to superficial zone compaction of 20% suggesting that the loss of superficial compressive and dynamic stiffness was not associated with changes in GAG density or GAG loss.

We showed that GAG loss did not occur during or immediately after injury but was delayed. The amount of GAG content and loss were initially small in the superficial zone, but by two days after injury, GAG loss had reached almost 20% of the entire content of the superficial

zone disks. Because control disks had lost only 10% of their GAG content, these results represent almost a two-fold increase of injury-induced superficial zone GAG loss. We investigated whether the zonal differences in GAG loss were related to zonal biosynthetic differences, possibly an attempt to repair ECM damage. However, our choice of injury did not affect the cellular biosynthesis significantly. Thus, it is unlikely that injury-induced GAG loss was increased by superficial biosynthetic activity.

Disruptions of the articular surface as large as 200μm had occurred after injury. Although we did not examine whether structural damage to single collagen fibrils had occurred, surface disruptions of that size were necessarily accompanied by damage to the local collagen network on a more global scale. Surface fissures such as those observed are related to failure of the collagen network due to the tensile stress of rapid impact loading(39). A recent study showed that injurious load led to a disrupted fiber orientation within lesions(40). Interestingly, that study showed that a high-enough load caused deeper collagen fibers to crimp by 10°. This amount is comparable to the change of 13.6° which we observed in deeper zones disks (Figure 5). The crimping of collagen fibers is thought to decrease articular cartilage vulnerability to shear-induced damage by lowering the effective strain on individual collagen fibrils(15). Buckley et al. also found a shear modulus minimum at about 125μm depth from the surface of immature cartilage(15), a depth which was included within our superficial zone disks suffering severe damage. Indeed, we observed a crimping of collagen fibers only in the deeper zones, which remained intact, but not in the damaged superficial zone, which suffered severe damage. Thus, the absence of crimping, possibly do to the slightly oblique orientation of the collagen fibers near the surface, as well as the shear weakness of the superficial zone, may strongly contribute to its vulnerability. Whereas crimping has been shown for adult cartilage(41), we demonstrated that collagen crimping also occurred in the deep zones of injured immature cartilage and may have contributed to the ability of these zones to maintain structural and functional integrity under injurious compression.

Another contributing factor to the observed biomechanical failure of the superficial zone may be associated with permeability changes due to alterations of the superficial collagen fibrils(42). However, our data showed that the angle between the immature articular surface and its superficial collagen fibers was approximately 10°, and that injury did not flatten or crimp those fibers any further. Thus, changes in the superficial collagen fiber orientation and associated permeability changes unlikely contributed to the biomechanical impairment of the superficial zone. In contrast, the dynamic stiffness was, after injury, to a small amount resolvable; the remaining dynamic stiffness was possibly derived from surface areas in which fluid had remained pressurized by compaction.

Structural damage of the immature superficial zone may be the most important observation to explain its biomechanical failure. Other studies also suggest that GAG loss may be related to mechanical ECM damage rather than to cell-mediated processes involving biosynthesis(24). We further quantified these surface disruptions and showed that they occurred in approximately 53% of the injured superficial zone disks. Although the occurring damage was equally visible histologically and in DEI-x-rays, we showed that only texture analysis of DEI-images was suitable to quantify a decreased structural regularity within regions with surface disruption. Because it was not possible to perform texture analysis of histological sections containing surface splits, we visualized the surface damage with DEI allowing further textural quantification. Importantly, texture analysis of histological sections of seemingly intact surface areas suggested additional structural damage in microscopically intact surface areas. Thus, structural damage of both histologically compromised and, surprisingly, histologically intact immature surface regions had occurred and likely caused biomechanical failure.

Texture analysis is a continuously refined image analysis method that is applied not only in fields such as geography, satellite image analysis, and paleontology, but also in the medical community. In the field of musculoskeletal research, texture analysis was applied to quantify tendon ultrasound signals(43) and muscle MR images(44) but not to investigate articular cartilage. In images, texture analysis is based on quantification of local contrast (gray-level-differences) and spatial structure. Whereas various methods perform image gray-level-analysis, we used the gray level co-occurrence-matrix(23), which assesses the relative frequencies of gray-level-pixel-pairs separated by a distance d in the direction θ, thus forming a relative displacement vector (d, θ) stored as a matrix which can be used to extract statistical texture. Haralick suggested 14 features(23), of which we used ASM (texture regularity), entropy (irregularity), and IDM (homogeneity) to quantify the texture information of chondrocytes and surrounding ECM. After injury, compaction of histologically intact samples had led to significantly decreased texture regularity and homogeneity and increased irregularity demonstrating that local contrast and spatial structure were altered by injurious compaction. Thus, texture analysis may prove to be a valuable tool in studies concerned with articular cartilage integrity.

The question arises as to further consequences of superficial ECM damage. In adult human joints, the superficial chondrocytes display distinct organizational patterns, whose joint-type-correlations may suggest a role in mechano-sensing(45). In early OA, they undergo a distinct spatial re-organization distant from OA lesions, possibly to recruit metabolically active units as attempt to repair focal damage(46). In addition, other unique characteristics such as synthesis of lubricative(47) and cell death regulative gene products(48), tissue-fluid boundary functions, and the presence of cells with stem cell properties(49) indicate vital roles of the superficial zone, which may be compromised by structural damage and thus advance the progression of surface-confined damage to degradation and possibly early OA.

It is important to discuss whether cutting the cartilage cylinders into two disks had any effect on the biomechanical results. We compared the biomechanical properties of thick deeper zones disks with significantly thinner deeper zones disks. Importantly, their equilibrium moduli were not significantly different. Thus, comparing cartilage disks with different thicknesses did not have any measurable effects on the biomechanical properties.

In conclusion, we exposed a vulnerability of the soft immature superficial zone to compressive injury. Injury caused articular surface damage including disruption, severe compaction, and textural alteration of seemingly intact areas. Consequences of the damage were the immediate loss of the biomechanical functioning of the superficial zone, followed by a delayed onset of GAG loss, whose relative amounts were highest within the superficial zone. GAG loss, which is a hallmark in the development of OA(50), did not contribute to the immediate biomechanical failure of the superficial zone. Nevertheless, it may cause additional softening of surface and underlying tissue, which may favor further damage or degradation and may contribute to the development of early secondary OA. Ongoing studies in our laboratory analyzing the human superficial zone focus on a comparable vulnerability.

Acknowledgments

References

1. Furukawa T, Eyre DR, Koide S, Glimcher MJ. Biochemical studies on repair cartilage resurfacing experimental defects in the rabbit knee. J Bone Joint Surg Am. 1980; 62(1):79–89. [PubMed: 7351420]

NIH-PA Author Manuscript

2. Brittberg M, Peterson L, Sjogren-Jansson E, Tallheden T, Lindahl A. Articular cartilage engineering with autologous chondrocyte transplantation. A review of recent developments. J Bone Joint Surg Am. 2003; 85-A 3:109–15. [PubMed: 12925617]

3. Nehrer S, Spector M, Minas T. Histologic analysis of tissue after failed cartilage repair procedures. Clin Orthop Relat Res. 1999; (365):149–62. [PubMed: 10627699]

4. Davis MA, Ettinger WH, Neuhaus JM, Cho SA, Hauck WW. The association of knee injury and obesity with unilateral and bilateral osteoarthritis of the knee. Am J Epidemiol. 1989; 130(2):278–88. [PubMed: 2750727]

5. Quinn TM, Grodzinsky AJ, Hunziker EB, Sandy JD. Effects of injurious compression on matrix turnover around individual cells in calf articular cartilage explants. J Orthop Res. 1998; 16(4):490–9. [PubMed: 9747792]

6. Repo RU, Finlay JB. Survival of articular cartilage after controlled impact. J Bone Joint Surg Am. 1977; 59(8):1068–76. [PubMed: 591538]

7. Loening AM, James IE, Levenston ME, Badger AM, Frank EH, Kurz B, et al. Injurious mechanical compression of bovine articular cartilage induces chondrocyte apoptosis. Arch Biochem Biophys. 2000; 381(2):205–12. [PubMed: 11032407]

8. Morel V, Quinn TM. Cartilage injury by ramp compression near the gel diffusion rate. J Orthop Res. 2004; 22(1):145–51. [PubMed: 14656673]

9. Venn M, Maroudas A. Chemical composition and swelling of normal and osteoarthrotic femoral head cartilage. I. Chemical composition. Ann Rheum Dis. 1977; 36(2):121–9. [PubMed: 856064]

10. Hunziker, EB. Articular cartilage structure in humans and experimental animals. In: Kuettner, KE.; Schleyerbach, R.; Peyron, JG.; Hascall, VC., editors. Articular Cartilage and Osteoarthritis. New York: Raven Press; 1992. p. 183-199.

11. Schinagl RM, Gurskis D, Chen AC, Sah RL. Depth-dependent confined compression modulus of full-thickness bovine articular cartilage. J Orthop Res. 1997; 15(4):499–506. [PubMed: 9379258]

12. Ewers BJ, Dvoracek-Driksna D, Orth MW, Haut RC. The extent of matrix damage and chondrocyte death in mechanically traumatized articular cartilage explants depends on rate of loading. J Orthop Res. 2001; 19(5):779–84. [PubMed: 11562121]

13. Chen CT, Bhargava M, Lin PM, Torzilli PA. Time, stress, and location dependent chondrocyte death and collagen damage in cyclically loaded articular cartilage. J Orthop Res. 2003; 21(5):888–98. [PubMed: 12919878]

14. Klein TJ, Chaudhry M, Bae WC, Sah RL. Depth-dependent biomechanical and biochemical properties of fetal, newborn, and tissue-engineered articular cartilage. J Biomech. 2007; 40(1):182–90. [PubMed: 16387310]

15. Buckley MR, Gleghorn JP, Bonassar LJ, Cohen I. Mapping the depth dependence of shear properties in articular cartilage. J Biomech. 2008; 41(11):2430–7. [PubMed: 18619596]

16. Oeppen RS, Connolly SA, Bencardino JT, Jaramillo D. Acute injury of the articular cartilage and subchondral bone: a common but unrecognized lesion in the immature knee. AJR Am J Roentgenol. 2004; 182(1):111–7. [PubMed: 14684522]

17. Kurz B, Jin M, Patwari P, Cheng DM, Lark MW, Grodzinsky AJ. Biosynthetic response and mechanical properties of articular cartilage after injurious compression. J Orthop Res. 2001; 19(6):1140–6. [PubMed: 11781016]

18. Frank EH, Jin M, Loening AM, Levenston ME, Grodzinsky AJ. A versatile shear and compression apparatus for mechanical stimulation of tissue culture explants. J Biomech. 2000; 33(11):1523–7. [PubMed: 10940414]

19. Sui Y, Lee JH, DiMicco MA, Vanderploeg EJ, Blake SM, Hung HH, et al. Mechanical injury potentiates proteoglycan catabolism induced by interleukin-6 with soluble interleukin-6 receptor and tumor necrosis factor alpha in immature bovine and adult human articular cartilage. Arthritis Rheum. 2009; 60(10):2985–96. [PubMed: 19790045]

20. Farndale RW, Buttle DJ, Barrett AJ. Improved quantitation and discrimination of sulphated glycosaminoglycans by use of dimethylmethylene blue. Biochim Biophys Acta. 1986; 883(2):173–7. [PubMed: 3091074]

21. Jones KB, Inoue N, Tis JE, McCarthy EF, McHale KA, Chao EY. Quantification of the microstructural anisotropy of distraction osteogenesis in the rabbit tibia. Iowa Orthop J. 2005; 25:118–22. [PubMed: 16089083]

22. Muehleman C, Li J, Wernick M, Brankov J, Kuettner K, Zhong Z. Yes, you can see cartilage with X-rays; diffraction enhanced X-ray imaging for soft and hard tissues. J Musculoskelet Neuronal Interact. 2004; 4(4):369–70. [PubMed: 15758263]

23. Haralik RM, Shanmugan K, Disstein I. Textural Features for image classification. IEEE Trans Syst, Man Cybernet. 1973; SMC-3:610–621.

24. DiMicco MA, Patwari P, Siparsky PN, Kumar S, Pratta MA, Lark MW, et al. Mechanisms and kinetics of glycosaminoglycan release following in vitro cartilage injury. Arthritis Rheum. 2004; 50(3):840–8. [PubMed: 15022326]

25. Mollenhauer J, Aurich ME, Zhong Z, Muehleman C, Cole AA, Hasnah M, et al. Diffraction-enhanced X-ray imaging of articular cartilage. Osteoarthritis Cartilage. 2002; 10(3):163–71. [PubMed: 11869076]

26. Muehleman C, Chapman LD, Kuettner KE, Rieff J, Mollenhauer JA, Massuda K, et al. Radiography of rabbit articular cartilage with diffraction-enhanced imaging. Anat Rec A Discov Mol Cell Evol Biol. 2003; 272(1):392–7. [PubMed: 12704696]

27. Li J, Zhong Z, Lidtke R, Kuettner KE, Peterfy C, Aliyeva E, et al. Radiography of soft tissue of the foot and ankle with diffraction enhanced imaging. J Anat. 2003; 202(5):463–70. [PubMed: 12739623]

28. Li J, Williams JM, Zhong Z, Kuettner KE, Aurich M, Mollenhauer J, et al. Reliability of diffraction enhanced imaging for assessment of cartilage lesions, ex vivo. Osteoarthritis Cartilage. 2005; 13(3):187–97. [PubMed: 15727884]

29. Grodzinsky AJ. Electromechanical and physicochemical properties of connective tissue. Crit Rev Biomed Eng. 1983; 9(2):133–99. [PubMed: 6342940]

30. Armstrong CG, Mow VC. Variations in the intrinsic mechanical properties of human articular cartilage with age, degeneration, and water content. J Bone Joint Surg Am. 1982; 64(1):88–94. [PubMed: 7054208]

31. Wilson W, van Donkelaar CC, van Rietbergen B, Huiskes R. A fibril-reinforced poroviscoelastic swelling model for articular cartilage. J Biomech. 2005; 38(6):1195–204. [PubMed: 15863103]

32. Soltz MA, Ateshian GA. Interstitial fluid pressurization during confined compression cyclical loading of articular cartilage. Ann Biomed Eng. 2000; 28(2):150–9. [PubMed: 10710186]

33. Gu WY, Yao H, Huang CY, Cheung HS. New insight into deformation-dependent hydraulic permeability of gels and cartilage, and dynamic behavior of agarose gels in confined compression. J Biomech. 2003; 36(4):593–8. [PubMed: 12600349]

34. Mow VC, Holmes MH, Lai WM. Fluid transport and mechanical properties of articular cartilage: a review. J Biomech. 1984; 17(5):377–94. [PubMed: 6376512]

35. Federico S, Herzog W. On the anisotropy and inhomogeneity of permeability in articular cartilage. Biomech Model Mechanobiol. 2007

36. Maroudas A. Biophysical chemistry of cartilaginous tissues with special reference to solute and fluid transport. Biorheology. 1975; 12(3-4):233–48. [PubMed: 1106795]

37. Chen SS, Falcovitz YH, Schneiderman R, Maroudas A, Sah RL. Depth-dependent compressive properties of normal aged human femoral head articular cartilage: relationship to fixed charge density. Osteoarthritis Cartilage. 2001; 9(6):561–9. [PubMed: 11520170]

38. Mansour JM, Mow VC. The permeability of articular cartilage under compressive strain and at high pressures. J Bone Joint Surg Am. 1976; 58(4):509–16. [PubMed: 1270471]

39. Kafka V. Surface fissures in articular cartilage: new concepts, hypotheses and modeling. Clin Biomech (Bristol, Avon). 2002; 17(1):73–80.

40. Moger CJ, Arkill KP, Barrett R, Bleuet P, Ellis RE, Green EM, et al. Cartilage collagen matrix reorientation and displacement in response to surface loading. J Biomech Eng. 2009; 131(3): 031008. [PubMed: 19154067]

41. Thambyah A, Broom N. Micro-anatomical response of cartilage-on-bone to compression: mechanisms of deformation within and beyond the directly loaded matrix. J Anat. 2006; 209(5): 611–22. [PubMed: 17062019]

42. Wu JP, Kirk TB, Zheng MH. Study of the collagen structure in the superficial zone and physiological state of articular cartilage using a 3D confocal imaging technique. J Orthop Surg Res. 2008; 3:29. [PubMed: 18637164]

43. Collinger JL, Gagnon D, Jacobson J, Impink BG, Boninger ML. Reliability of quantitative ultrasound measures of the biceps and supraspinatus tendons. Acad Radiol. 2009; 16(11):1424–32. [PubMed: 19596592]

44. Mahmoud-Ghoneim D, Cherel Y, Lemaire L, de Certaines JD, Maniere A. Texture analysis of magnetic resonance images of rat muscles during atrophy and regeneration. Magn Reson Imaging. 2006; 24(2):167–71. [PubMed: 16455405]

45. Rolauffs B, Williams JM, Grodzinsky AJ, Kuettner KE, Cole AA. Distinct horizontal patterns in the spatial organization of superficial zone chondrocytes of human joints. J Struct Biol. 2008; 162(2):335–44. [PubMed: 18325787]

46. Rolauffs B, Williams JM, Aurich M, Grodzinsky AJ, Kuettner KE, Cole AA. Proliferative remodeling of the spatial organization of human superficial chondrocytes distant from focal early osteoarthritis. Arthritis Rheum. 2010; 62(2):489–498. [PubMed: 20112377]

47. Schumacher BL, Hughes CE, Kuettner KE, Caterson B, Aydelotte MB. Immunodetection and partial cDNA sequence of the proteoglycan, superficial zone protein, synthesized by cells lining synovial joints. J Orthop Res. 1999; 17(1):110–20. [PubMed: 10073655]

48. Khan IM, Salter DM, Bayliss MT, Thomson BM, Archer CW. Expression of clusterin in the superficial zone of bovine articular cartilage. Arthritis Rheum. 2001; 44(8):1795–9. [PubMed: 11508431]

49. Tallheden T, Brittberg M, Peterson L, Lindahl A. Human articular chondrocytes--plasticity and differentiation potential. Cells Tissues Organs. 2006; 184(2):55–67. [PubMed: 17361078]

50. Kuettner KE, Cole AA. Cartilage degeneration in different human joints. Osteoarthritis Cartilage. 2005; 13(2):93–103. [PubMed: 15694570]
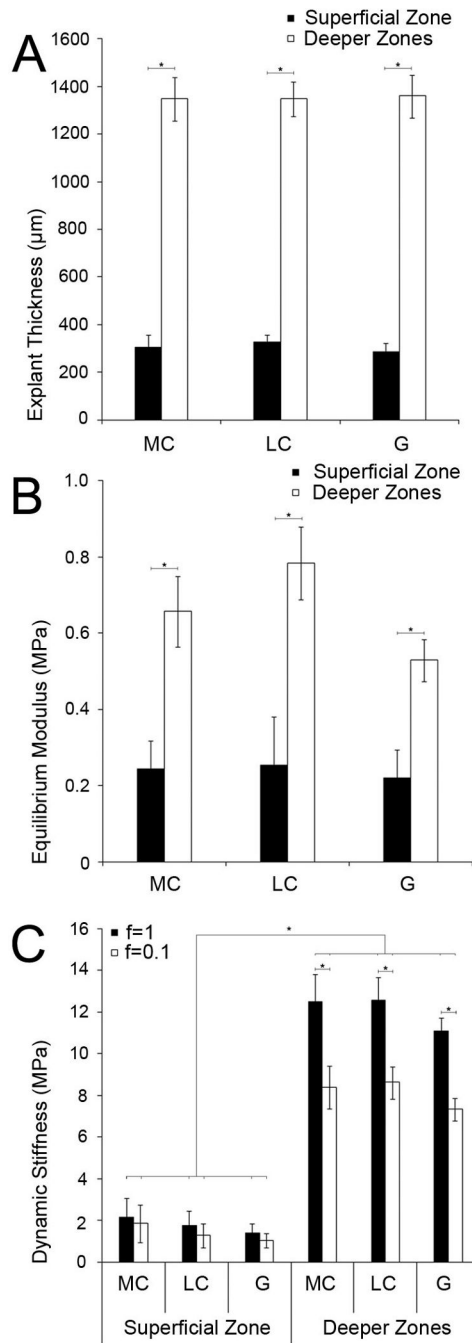
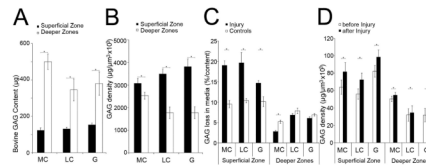**Figure 1. Characterization of cartilage disks before injury**
(A) Thickness of superficial zone and deeper zones disks of the medial, lateral condyle and the patella-femoral groove. (B) Equilibrium modulus of superficial zone and deeper zones disks. (C) Dynamic stiffness of superficial zone and deeper zones disks.
(A, B, C) Each group of superficial zone disks: $n \geq 7$; each group of deeper zones disks: $n \geq 12$. MC = medial condyle, LC = lateral condyle, G = patellofemoral groove.
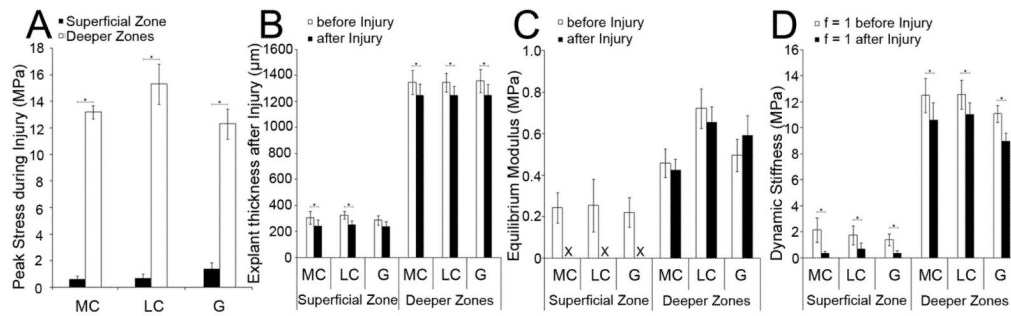
**Figure 2. Changes in disk properties after injury**
(A) Peak stress during injury. (B) Disk thickness before/after injury. (C) Equilibrium modulus before/after injury. The X indicates that the superficial zone equilibrium modulus was not resolvable after injury. (D) Dynamic stiffness at a frequency of f = 1 before/after injury. (A) Superficial zone and deeper zones disks: n ≤ 6 samples/group. (B, C, D) Superficial zone disks: n ≥ 7 samples/group; deeper zones disks: n ≥ 12 samples/group.

Figure 3. Biochemical characterization

(A) GAG content (µg) of superficial zone and deeper zones disks of the medial, lateral condyle and the patellofemoral groove before injury. (B) GAG density ($\mu g/\mu m^3$) $\times 10^6$ of superficial zone and deeper zones control disks. (C) GAG loss into the media (% of GAG content) after 48 hours of control and injured disks of the superficial zone and deeper zones. (D) GAG density ($\mu g/\mu m^3$) $\times 10^6$ of superficial zone and deeper zones disks before and 5 minutes after injury.

(A, B) Each group of superficial zone and deeper zones disks: n ≥ 12 samples. (C, D) Each group of superficial zone and deeper zones disks: n ≥ 8 samples.
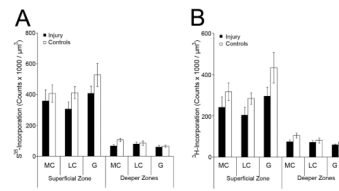
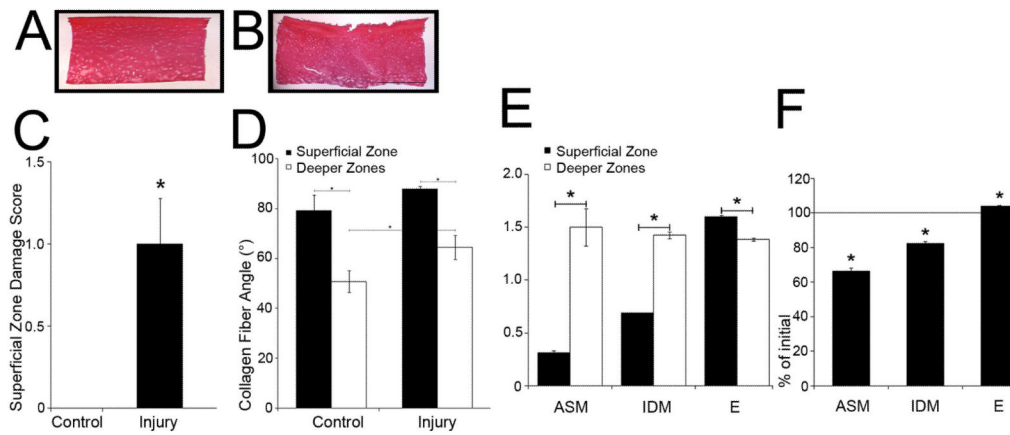**Figure 4. Biosynthesis after injury**

(A) Scintillation counts after radiolabel incorporation of $^{35}SO_4^{-2}$, and (B) ^{3}H-proline 24 hours after injury.

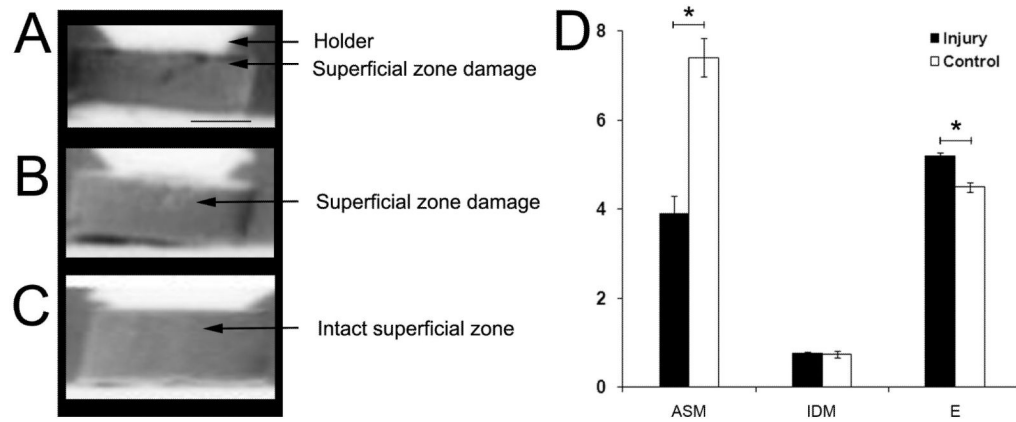(A, B) Each group of superficial zone and deeper zones disks: n ≥ 6 samples.

Figure 5. Histology, superficial zone damage score, collagen angles, and texture analysis of injured/control disks

Representative samples of 6μm sections of control (A) and injured disks (B). Note the large surface ECM disruption of 207 μm width / 162 μm depth. Scale bar, 1000 μm. (C) Damage score of the superficial zone of injured/control disks after paraffin embedding/staining with Safranin O/fast green. Grade 0=normal appearing cartilage with proper staining in each zone except the intact superficial zone with the surface showing no signs of damage; Grade 1=minimal surface damage with isolated disruptions; Grade 2=moderate surface damage with widespread disruption; Grade 3=minimal permanent compression; Grade 4=permanent compression to approximately ≥ 30% of the original disk thickness. (D) Angle (°) between collagen fibers and longitudinal disk axis of injured and control disks. (E) Texture analysis of zonal differences of control disks. ASM=Angular Second Moment, IDM=Inverse Difference Moment, E=Entropy. (F) The percent change in texture analysis measures after injury.

(C) Each group of superficial zone and deeper zones disks: n ≥ 17 samples. (D) Control group: n ≥ 7 samples, Injury group: n ≥ 10 samples. (E, F) Each group: n ≥ 6 samples.

Figure 6. Diffraction-Enhanced X-Ray Imaging (DEI) and texture analysis of injured and control disks
Representative DEI-images of two disks with damage to the superficial zone showing (A) an isolated fissure and (B) slight damage, and (C) image of the intact superficial zone of a control disk. Scale bar, 1000μm. (D) Texture analysis of ROIs containing the superficial zone of injured and control disks. ASM=Angular Second Moment, IDM=Inverse Difference Moment, E=Entropy. Each group of superficial zone and deeper zones disks: n ≥ 5 samples.